Accepted Manuscript

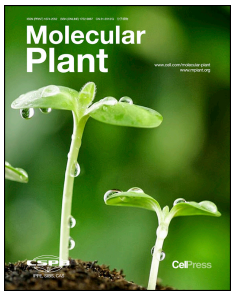

Circadian Evening Complex represses Jasmonate-induced leaf senescence in *Arabidopsis*

Yuanyuan Zhang, Yan Wang, Hua Wei, Na Li, Wenwen Tian, Kang Chong, Lei Wang

PII: S1674-2052(18)30020-0
DOI: 10.1016/j.molp.2017.12.017
Reference: MOLP 573

To appear in: *MOLECULAR PLANT*
Accepted Date: 27 December 2017

Please cite this article as: **Zhang Y., Wang Y., Wei H., Li N., Tian W., Chong K., and Wang L.** (2018). Circadian Evening Complex represses Jasmonate-induced leaf senescence in *Arabidopsis*. Mol. Plant. doi: 10.1016/j.molp.2017.12.017.

Circadian Evening Complex represses Jasmonate-induced leaf senescence in *Arabidopsis*

Yuanyuan Zhang[1], Yan Wang[1,2], Hua Wei[1,2], Na Li[1,2], Wenwen Tian[1,2], Kang Chong[1,3] and Lei Wang[1,2,*]

[1]Key Laboratory of Plant Molecular Physiology, CAS Center for Excellence in Molecular Plant Sciences, Institute of Botany, Chinese Academy of Sciences, Beijing 100093, China.

[2]University of Chinese Academy of Sciences, Beijing 100049, China.

[3]National Center for Plant Gene Research, Beijing 100093, China

[*]Corresponding author: wanglei@ibcas.ac.cn

Running title: Circadian clock regulates leaf senescence

Short Summary：

Evening Complex (EC), a core component of circadian oscillator, negatively regulates leaf senescence in *Arabidopsis thaliana*. EC directly binds the promoter of *MYC2*, which encodes a key activator of JA-induced leaf senescence, and represses its expression. Collectively, our results reveal a critical molecular mechanism illustrating how the core component of circadian clock gates JA signaling to regulate leaf senescence.

Abstract

Plants initiate leaf senescence to reallocate energy and nutrients from the aging to developing tissues for optimizing growth fitness and reproduction at the end of growing season or under stress. Jasmonate (JA), a lipid-derived phytohormone, is known as an important endogenous singal in inducing leaf senescence. However, whether and how circadian clock gates JA signaling to induce leaf senescence in plants remains elusive. In this study, we show that the Evening Complex (EC), a core component of circadian oscillator, negatively regulates leaf senescence in *Arabidopsis thaliana*. Transcriptomic profiling analysis reveals that EC is closely involved in JA signaling and response, consistent with accelerated leaf senescence unanimously displayed by EC mutants upon JA induction. We found that EC directly binds the promoter of *MYC2*, which encodes a key activator of JA-induced leaf senescence, and represses its expression. Genetic analysis further demonstrated that the accelerated JA-induced leaf senescence in EC mutants is abrogated by *myc2 myc3 myc4* triple mutation. Collectively, these results reveal a critical molecular mechanism illustrating how the core component of circadian clock gates JA signaling to regulate leaf senescence.

Key words: Circadian clock/ Evening Complex/ JA signal/ leaf senescence/ MYC2

Introduction

As an ubiquitous molecular time-keeping mechanism, circadian clock provides an adaptive advantage to higher plants by synchronizing internal growth behaviors with external daily changing environments (Sanchez & Kay, 2016). The core oscillator function of plant circadian clock is based on transcriptional–translational feedback loops, which constitute a critical part of the self-sustaining oscillator (Greenham & McClung, 2015; Hsu & Harmer, 2014). Evening complex (hereafter as EC), comprised of EARLY FLOWERING3 (ELF3), EARLY FLOWERING 4 (ELF4) and LUX ARRHYTHMO (LUX), plays essential roles in plant circadian clock, as mutation of any EC components leads to circadian arrhythmia (Helfer et al, 2011; Sanchez & Kay, 2016). LUX is a single MYB domain containing SHAQYF-type GARP transcription factor, targeting GATWCG promoter element (LUX binding site, LBS) through its specific DNA-binding domain (Helfer et al, 2011; Nusinow et al, 2011). ELF3 and ELF4 are nuclear proteins with unidentified biochemical function, whereas ELF3 functions as an adaptor between LUX and ELF4, thus forming a ternary transcriptional repression complex. It has been demonstrated that EC represses the expression of *PRR7*, *PRR9*, *GIGANTEA* and *LUX* itself (Chow et al, 2012; Helfer et al, 2011; Nusinow et al, 2011) within the circadian core oscillator.

EC is a critical component of core oscillator in regulating circadian outputs (Mizuno et al, 2014). For example, EC directly regulates the expression of *PHYTOCHROME INTERACTING FACTOR 4* (*PIF4*) and *PIF5* to gate the hypocotyl growth in early evening (Nusinow et al, 2011). Interestingly, ELF3 also regulates hypocotyl elongation in an EC-independent manner by interacting with PIF4 and impeding its transcriptional activation of the downstream target genes (Nieto et al, 2015). In addition, *elf3* mutant, but not *elf4* and *lux* mutants, displays a dark-induced early leaf-senescence phenotype, implying that ELF3 can affect leaf senescence independent of EC-mediated transcriptional repression activity (Sakuraba et al, 2014). However, it remains unclear if EC-mediated transcriptional repression is still involved in leaf senescence governed by other cues.

As the last and inevitable stage of leaf development, leaf senescence is under the control

of highly coordinated cellular processes to trigger the reallocation of nutrients and energy to developing tissues or storage organs (Gan & Amasino, 1995; Lim et al, 2007). Proper timing of the onset of leaf senescence is critical for seed yield, fruit ripening and biomass production (Lim et al, 2007; Wu et al, 2012). A concerted cellular event is triggered upon leaf senescence, such as rapid chlorophyll degradation, increase of membrane ion leakage, and eventually the decline of photochemical biosynthesis (Qi et al, 2015). These biochemical processes are often associated with an up-regulation of many senescence-associated genes, such as *SENESCENCE-ASSOCIATED GENE12* (*SAG12*), *SAG13*, *SAG29*, *SAG113*, *SENESCENCE4* (*SEN4*), and down-regulation of photosynthetic gene, such as *RIBULOSE BISPHOSPHATE CARBOXYLASE SMALL CHAIN* (*RBCS*) (Gan & Amasino, 1995; Hortensteiner, 2006; Park et al, 1998; Qi et al, 2015; Weaver et al, 1998). Although leaf senescence is basically governed by the developmental cues, it is also tightly regulated by various external and internal signals through specific pathways, such as darkness, drought, high salinity, pathogen infection and phytohormones (Lim et al, 2007; Qi et al, 2015). Leaf senescence is also regulated by a distinct set of plant hormones, including ethylene, ABA, SA and JA (Miao & Zentgraf, 2007; Qi et al, 2015; Qiu et al, 2015; Zhao et al, 2016).

JA, a class of lipid-derived phytohormones, has been well documented in regulating leaf senescence (He et al, 2002). The JA signal is perceived by CORONATINE INSENSITIVE1 (COI1), a F-box domain containing protein, which results in the recruitment of jasmonate ZIM-domain (JAZ) transcriptional repressors for ubiquitination and degradation (Thines et al, 2007; Xie et al, 1998; Xu et al, 2002), and de-repression of various downstream JA responsive transcription factors, including MYC2, MYC3, and MYC4 (Chen et al, 2011; Fernandez-Calvo et al, 2011; Qi et al, 2015). The IIIe bHLH transcription factor family MYC2, 3, 4 redundantly binds *SAG29* promoter and activates its expression, leading to the activation of JA-induced leaf senescence (Qi et al, 2015). The NAC transcriptional factors, *ANAC019*, *ANAC055* and *ANAC072*, are also direct targets of MYC2 in mediating JA-induced leaf senescence (Bu et al, 2008; Zhu et al, 2015).

A few lines of evidence have revealed the involvement of circadian clock in regulating JA signaling. First, the accumulation of jasmonates is in-phase peaking at the middle of

subjective day, well in line with anticipated peak of circadian-mediated insect feeding behavior (Goodspeed et al, 2013; Goodspeed et al, 2012). Second, plant circadian clock driven time-of-day susceptibility to necrotrophic fungal pathogen, *Botrytis cinerea*, is mediated by JA signaling (Ingle et al, 2015). Third, TIME FOR COFFEE (TIC), a circadian-clock mediator, acts as a negative regulator in JA signaling by repressing MYC2 protein accumulation at the post-translational level (Shin et al, 2012). Intriguingly, the *MYC2* transcription is also regulated by circadian clock, although the mechanism is unknown (Shin et al, 2012). In this study, we found that EC, a circadian clock core complex, is involved in JA signaling and response. Loss-of-function of EC results in JA-dependent early leaf senescence. EC directly regulates JA-induced leaf senescence by binding to the *MYC2* promoter and repressing its transcription. Our findings have revealed a novel molecular mechanism underlying circadian gated leaf senescence mediated by JA.

Results

EC acts as a negative regulator of leaf senescence

The EC mutants including *elf3*, *elf4* and *lux* share a few common phenotypes, such as arrhythmic circadian period, long hypocotyl, and early flowering (Nusinow et al, 2011). Interesting, ELF3 inhibit dark-induced leaf senescence through post-translational suppression of PIF4 and PIF5, independent of EC transcriptional repression activity. To determine if EC could affect leaf senescence under physiological conditions, we grew *elf3-1 elf4-209* double mutant, *lux-6* (Supplemental Figure 1), and other EC mutants under long day condition with 16 h light period. As reported previously, all the EC mutants displayed long hypocotyl, long petiole and early flowering phenotypes. No additive phenotypes were observed in *elf3-1 elf4-209* double mutant (Supplemental Figure 1), in line with the fact that ELF3 and ELF4 functioning in the same complex (Nusinow et al, 2011). The *lux-6* mutant also showed an arrhythmic circadian period like other EC mutants (Supplemental Figure 1H). Notably, the tips of rosette leaves in *elf3-1, elf4-209, elf3-1 elf4-209* and *lux-6* became yellow but not in the wild-type Col-0 in 5-week-old plants (Figure 1A). To confirm the early leaf senescence phenotypes, the ChlF (Chlorophyll Fluorescence) parameters were measured to estimate the effective quantum yield of photochemical energy conversion in PSII (ΦPSII) (Mishra et al,

2016). Indeed, the PSII efficiencies in EC mutants were significantly lower than that in Col-0 (Figure 1B and C). Moreover, the chlorophyll contents of the third and fourth leaves were much lower in EC mutants than that in Col-0 (Figure 1D), while the ion leakage was higher in EC mutants than in Col-0 (Figure 1E). Compared to Col-0, the expression of photosynthetic genes, *RBCS* and *CAB1*, was dramatically reduced in leaves of EC mutants (Figure 1F and G). The expression of *SAG12*, a senescence marker gene which is not induced under stress conditions, was significantly increased in leaves of EC mutants. *lux-6* has the lowest induction of *SAG12* compared to *elf3-1* and *elf4-209* mutants and the double mutant, which might be due to *lux-6* itself is a weak allele of *LUX*. The low induction is in line with higher chlorophyll retention and lower ion leakage; however, down-regulation of RBCS is more severe in *lux-6* than in the other mutants, indicating that the different EC mutants have different impacts on the senescence program (Figure 1H). Taken together, the EC mutants unanimously displayed early leaf senescence, indicating EC may act as a negative element in leaf senescence regulatory network through its transcriptional repression activity, which is distinct form ELF3-dependent and EC-independent inhibition of PIF4 and PIF5 activities.

Transcriptome profiling analysis reveals links between EC and JA signaling

To explore potential mechanisms underlying EC-mediated leaf senescence, we conducted RNA-sequencing using 10-day-old *lux-6* and Col-0 seedlings. Two biological replicates were performed with the tissues harvested at ZT12, the peak expression time of EC components. In total, we found 978 differentially expressed genes (DEGs) in *lux-6* mutant compared to Col-0 with 2-fold cut-off (FDR<0.05). Among which 72.5% (709/978) was up-regulated, consistent with EC being a transcriptional repressor complex (Figure 2A, and Supplemental Dataset 1) (Nusinow et al, 2011). Functional assignment of the DEGs by GO enrichment analysis revealed a wide array of JA signaling-mediated biological processes, including response to biotic stimulus, immune response, camalexin and phytoalexin biosynthetic and metabolic processes, aging and jasmonic acid itself (Figure 2B and Supplemental Figure 2). The collection of senescence-regulatory genes (SRGs) in *Arabidopsis* comprised of 192 genes involved in various regulatory networks underlying leaf senescence (Supplemental Dataset 2) (Li et al., 2014; Sakuraba et al., 2014). Nearly 13% of the SRGs

(25/192, *p*=1.4e-7, hypergeometric test, Supplemental Figure 3A) was present in the DEGs in *lux-6* mutant. In line with *lux-6*'s early leaf senescence phenotypes, 19 out of the 25 SRGs (*p*=2.5e-6, hypergeometric test) were up-regulated, including *ORE1* (*ORESARA 1*), *NAP* and *MYC2* (Figure 2C), whereas only 6 SRGs (*p*=0.017, hypergeometric test) were down-regulated in *lux-6* mutant (Supplemental Figure 3B). In total, ca. 16 % senescence-promoting of SRGs (16/97, *p*=1.2e-7, hypergeometric test, Supplemental Figure 3C) were overlapped with the up-regulated genes in *lux-6* mutant. However, only 3 senescence-inhibiting SRGs (*p*=0.2, hypergeometric test) overlapped with the down-regulated genes in *lux-6* mutant (Supplemental Figure 3D). In *Arabidopsis*, there is a significant overlap (18 genes, ~10%) between 192 SRGs and 190 JA-responsive genes (Supplemental Figure 3E). Since GO enrichment analysis indicated that JA related biological processes were affected in *lux-6* mutant (Figure 2B), we found a significant number of DEGs (16, all up-regulated) in *lux-6* that overlapped with the 190 JA-responsive genes (*p*<1.1e-4, hypergeometric test) (Figure 2D).

Notably, *MYC2*, *WRKY70*, *JAZ7* and *LOX3* were found in both the 19 SAGs (Figure 2C) and 18 JA-responsive (Figure 2D) overlapping gene pools, implicating that EC might be involved in JA-induced leaf senescence. Consistent with this notion, *MYC2* and its downstream key factors involved in leaf senescence induction, such as *ANAC019*, *ANAC055* and *ANAC072* (Zhu et al, 2015), were up-regulated in *lux-6* mutant in RNA-seq analysis (Figure 2E-F). To validate the RNA-seq results, RT-qPCR (Supplemental Figure 4) was conducted to confirm the elevated expression of 6 genes in *lux-6* mutant. Taken together, results of the transcriptome profiling analysis suggested that EC might regulate JA induced leaf senescence via its transcriptional repression activity.

EC is involved in JA-induced leaf senescence

To substantiate the idea that EC may regulate JA induced leaf senescence, we comprehensively examined JA-induced leaf senescence in EC mutants such as *lux-6*, *elf3-1*, *elf4-209* and *elf3-1 elf4-209* using previously well-established protocols (Qi et al, 2015; Shan et al, 2011). We choose 3-weeks old Col-0, *lux-6*, *elf3-1*, *elf4-209* and *elf3-1 elf4-209* mutants to analyze the JA-induced leaf senescence phenotype, when senescence was still not initiated

in the EC mutant leaves (Supplemental Figure 5). Compared to the wild-type Col-0, *lux-6*, *elf3-1*, *elf4-209* and *elf3-1 elf4-209* mutants displayed accelerated JA-induced leaf senescence (Figure 3A). All the EC mutants treated with MeJA showed significant lower chlorophyll contents (Figure 3B and Supplemental Figure 6) and much higher levels of membrane ion leakage (Figure 3C). Consistent with the physiological phenotypes, the expression level of JA-induced SAGs (*SAG13*, *SAG29*, *SAG113*, and *SEN4*) was significantly up-regulated in EC mutants (Figure 3D-G). By contrast, the expression of photosynthetic related gene *RBCS* was appreciably reduced in EC mutants (Figure 3H).

The EC mutants including *elf3*, *elf4* and *lux* share a few characteristic phenotypes, such as circadian arrhythmia, long hypocotyl, and early flowering. Furthermore, ELF3 serves as a protein adaptor to recruit ELF4 and LUX respectively to form Evening Complex, whilst LUX acts as a transcription factor. To further validate the results of loss-of-function analyses, we generated *ELF3* and *LUX* overexpression lines; however, the protein level of *GFP-LUX* was relatively low (Supplemental Figure 7) probably due to the fact that EC can repress the expression of *LUX* itself (Helfer et al, 2011). Nevertheless, *ELF3* overexpression plants displayed late flowering phenotypes as previously reported (Covington et al, 2001; Kim et al, 2005; Nieto et al, 2015; Yu et al, 2008) (Supplemental Figure 8). In contrast to EC loss-of-function mutants, the 3-weeks old *ELF3* overexpression lines exhibited a staying-green phenotype with the MeJA treatment (Figure 4A), accompanied with higher chlorophyll contents and lower membrane ion leakages in the leaves (Figure 4B-C). Furthermore, the expression of *SAG13*, *SAG29*, *SAG113*, and *SEN4* was not significantly induced by MeJA, while the level of *RBCS* gene was notably higher (Figure 4D-H). As for the transgenic line *ELF3-OE* show a general shift in development with strongly delayed flowering, we also analyzed JA-induced leaf senescence phenotype of *ELF3* overexpression line and Col-0 when both lines have first flowers. Similarly, *ELF3* overexpression line exhibited a staying-green phenotype with the MeJA treatment (Supplemental Figure 9). Taken together, EC components appeared to be negative regulators in JA-induced leaf senescence.

EC directly gates JA-induced *MYC2* expression

To narrow down the underlying mechanisms of EC-mediated leaf senescence induced by

JA, we hypothesized that some of the crucial JA signaling components might be targets of EC. We searched the LUX binding site (LBS, GATWCG element) and found at least two LBS in the promoter of *COI1*, *JAZ1*, *MYC2*, *MYC3* and *MYC4* (Supplemental Table 1). The direct repressive roles of LUX protein on these genes were tested by using a transient expression analysis in *N. benthamiana*. Results showed that only *MYC2* was significantly repressed by LUX (Figure 5A-B). This result was further corroborated in *Arabidopsis* protoplast transient expression assay, in which LUX was capable of repressing the expression of *MYC2* but not *COI1* (Figure 5C). Given *MYC2* is considerably up-regulated in *lux-6* mutant (Figure 2E and Supplemental Figure 4A), and this up-regulation was especially evident in the evening upon MeJA-induction (Supplemental Figure 10), we proposed that *MYC2* is likely a direct target of EC in mediating JA-induced leaf senescence.

MYC2, together with MYC3, MYC4 has been shown as an accelerator of JA-induced leaf senescence, through competing with the bHLH IIId factors bHLH03, bHLH13, bHLH14 and bHLH17 in regulating *SAG29* expression (Qi et al, 2015). Consistently, we found that the *SAG29* expression was dramatically increased in JA-induced leaves of EC mutants (Figure 3E). However, we found that the *MYC2* promoter, rather than the *SAG29* promoter, was associated with LUX protein in a yeast one-hybrid assay (Figure 5D and Supplemental Figure 11). Two LBS, site 1 (GATTCT) and site 2 (GATATG), were found at -695 bp and -598 bp, respectively, upstream of *MYC2* start codon. To investigate whether EC repressed *MYC2* through direct binding to its promoter *in vivo*, chromatin immunoprecipitation (ChIP) assay using *pELF4:ELF4-HA* and *35S:GFP-LUX* transgenic lines was performed with tissue harvested at ZT 12. Significant enrichment was found in the *MYC2* promoter LBS site 2 region (Figure 5E). By contrast, there was less enrichment for LBS site 1 region and no enrichment for the region around start codon and the negative control *APX3* (Figure 5E). Taken together, we concluded that EC could bind *MYC2* promoter directly to suppress its transcription, which might be accounted for the effects of EC on JA-induced leaf senescence.

MYC2 is required for EC-mediated leaf senescence induced by JA

To determine if MYC2 was genetically required for EC-mediated leaf senescence induced by JA, we constructed *elf3-1 myc2* double mutant. Phenotypic analysis demonstrated

that the accelerated JA-induced leaf senescence in *elf3-1* mutant was reverted by introgression of *myc2* mutation, as evidenced by the delayed JA-induced leaf senescence in *elf3-1 myc2* double mutants (Figure 6A-C).

MYC2 belongs to the IIIe bHLH transcription factor family, which also includes MYC3 and MYC4. MYC2, 3, and 4 act redundantly in accelerating JA-induced leaf senescence, as *myc2 myc3 myc4* triple mutant showed greatest attenuation of JA-induced leaf senescence (Qi et al, 2015). As expected, the *lux-6 myc2 myc3 myc4* quadruple mutant exhibited a comparable staying-green phenotype just as *myc2 myc3 myc4* mutant when treated with MeJA (Figure 6 D-F). The chlorophyll contents and ion leakage in *lux-6 myc2 myc3 myc4* quadruple mutant were indistinguishable from the *myc2 myc3 myc4* mutants. Collectively, our genetic analyses unequivocally demonstrated that the IIIe bHLH factors are required for EC-mediated leaf senescence induced by JA.

Discussion

By synchronizing the daily and seasonal environmental timing cues, circadian clock coordinates a myriad of rhythmic biological processes to provide higher plants with adaptive advantage and fitness. However, the precise molecular mechanisms by which circadian clock regulates its output is largely unknown. EC components are not only essential for sustaining the core oscillator, but also involved in direct regulation of circadian outputs, such as rhythmic hypocotyl elongation (Nusinow et al, 2011). Among the EC components, ELF3 is known to regulate dark-induced leaf senescence through repressing PIF4 in an EC-independent manner (Liu et al, 2001; Nieto et al, 2015; Sakuraba et al, 2014). Unexpectedly, here we found that all EC mutants displayed precocious leaf senescence in plants grown under normal conditions. Transcriptome profiling analysis revealed that EC appeared to regulate JA signaling via its transcriptional repression activity. This idea is further supported by early leaf senescence upon JA induction in all EC mutants. We further identified *MYC2* as a direct transcriptional target of EC and demonstrated that *MYC2* acted downstream of EC genetically to mediate JA induced leaf senescence. Together, our findings have delineated a novel pathway in which leaf senescence is modulated by an EC-*MYC2* molecular module.

PIF4 and *PIF5* are direct targets of EC in regulating rhythmic hypocotyl elongation (Nusinow et al, 2011). The transcript level of *PIF4*/*PIF5* is significantly increased in our transcriptome profiling data (Supplemental Dataset1). Interestingly, ELF3, but not ELF4 and LUX, inhibited the dark-induced leaf senescence through repressing *PIF4*/*PIF5* (Sakuraba et al, 2014), implicating an independent role of ELF3 in regulating dark-induced leaf senescence. Interestingly, the *pif4 pif5* double mutant did not show early senescence phenotypes upon JA induction, suggesting that EC-mediated leaf senescence induced by JA does not involve *PIF4*/*PIF5* (Supplemental Figure 12). On the other hand, neither *myc2 myc3 myc4* triple mutant nor *MYC2 OE* plants showed any abnormal dark-induced leaf senescence phenotypes (Supplemental Figure 13). Hence, the dark- and JA-induced leaf senescence display a dichotomy in the complex senescence network and *MYC2* plays a specific role in mediating JA-induced leaf senescence regulated by EC.

As a final process in leaf development, leaf senescence is fundamentally important for plant fitness and reproductive growth (Lim et al, 2007). Here we delineate a JA-induced leaf senescence pathway under the regulation of EC via transcriptional repression of *MYC2*, implicating that EC components are important for maintaining the proper timing of leaf senescence (Figure 7). However, the early leaf senescence in EC mutants cannot be solely attributed to the impact on JA signaling. A number of master transcription factors involved in ABA and ethylene response were also found highly up-regulated in our transcriptome data, such as *MYB96*, *ABI5* and *ERF1/6/11* (Lee et al, 2016; Sakuraba et al, 2014). Furthermore, the transcript levels of *NAP* and *ORE1*, two key components of age-dependent and ethylene-mediated SAGs (Guo & Gan, 2006; Rauf et al, 2013), were appreciably up-regulated in *lux-6* mutant. The elevated expression of *NAP* and *ORE1* was further validated in senescent leaves of EC mutants (Supplemental Figure 14). Hence, it is possible that the early leaf senescence phenotype in EC mutants is an outcome caused by multiple senescence signaling pathways. In support of this notion, the combinatory effect by converging multiple downstream pathways has also been observed in PIF4/PIF5-mediated dark-induced leaf senescence. In that scenario, PIF4/PIF5 directly promotes *ORE1* transcription by binding to its promoter and also by indirectly regulating *ABI5* and *EIN3* expression via unknown

mechanisms. Hence this circuit similarly integrates ABA-, ethylene- and age-dependent senescence pathways. To further investigate whether EC directly repressed *NAP* expression, we performed a yeast one-hybrid assay and found that LUX was unable to bind *NAP* promoter (Supplemental Figure 15A-B). We also failed to detect a direct repressive role of LUX protein on *NAP* transcription (Supplemental Figure 15C-D). The transcript levels of *NAP* and *ORE1*, two key components of age-dependent and ethylene-mediated SAGs, were up-regulated slightly in *lux-6* mutant at earlier stages, but dramatically up-regulated in senescent leaves of EC mutants at later stages. It is plausible that EC directly represses *MYC2* at the transcription level, while indirectly affects *ORE1* and *NAP* expression through its circadian downstream target, such as *GI, LNK1, PRR7* or *PRR9.* At later stage, multiple senescence signaling pathways were all activated by transcriptional cascade and converged to regulate *ORE1* and *NAP* expression (Chow et al, 2012; Herrero et al, 2012; Mizuno et al, 2015). This hypothesis awaits further investigation.

It has long been known that JA signaling pathway is under an intimate control of endogenous circadian oscillators. First, jasmonates accumulation is circadian regulated, peaking in the middle of the day and lowermost at night (Goodspeed et al, 2012). Second, JA-responsive genes are preferentially expressed in the morning according to pervious microarray data (Covington et al, 2008). Third, accumulation of MYC2 protein is repressed at post-translational level by TIC (TIME FOR COFFEE), a crucial circadian component with unknown biochemical function, providing time-of-day regulation of jasmonate signaling in *Arabidopsis* (Shin et al, 2012). Finally, the timing of JA accumulation and signaling is tightly associated with the defense of biotic stresses, including insect and necrotrophic fungal pathogen (Goodspeed et al, 2013; Goodspeed et al, 2012; Ingle et al, 2015). Despite these previous findings, the transcriptional link between the core oscillator and JA signaling is still lacking. Our findings here on EC-*MYC2*'s role in JA-induced leaf senescence fills this knowledge gap. MYC2 acts as a positive regulator of senescence via activating its targets such as *SAG29, PAO* and *ANAC019/055/072* (Qi et al, 2015; Zhu et al, 2015). The Evening Complex directly binds to *MYC2* promoter and represses its transcription to modulate JA-induced leaf senescence. In addition, the JA accumulation was reduced in EC mutants

which might have caused by an uncharacterized feedback regulation (Figure 7A). Finally, the abundance of EC complex peaks at night and represses its targets, consistent with the fact that JA-responsive genes are mainly expressed in the morning (Covington et al, 2008). The dynamic control of *MYC2* expression by circadian components appears to be an important mechanism in multiple biological processes. The counterpart that involved in *MYC2* activation remains to be an interesting topic for future investigation.

Materials and Methods

Plant materials and growth conditions

The *Arabidopsis* seeds were sterilized with 10% NaClO for 10 min, then plated on Murashige and Skoog medium (Sigma-Aldrich) with 3% sucrose, stratified at 4°C for 2 d, then transferred to a grow housing chamber with 12 h light /12 h dark or 16 h light/8 h dark as indicated.

Chlorophyll measurement

Chlorophyll measurement was performed as described before (Qi et al, 2015; Sakuraba et al, 2014). The weight of detached leaves was record as W. For chlorophyll extraction, leaves were incubated in 80% acetone (v/v) in the dark, and the volume was recorded as V. Absorbance was measured at 645 and 663 nm, and the chlorophyll contents were calculated with the formula of (8.02A663+20.21A645)*V/W.

Measurement of membrane ion leakage

For membrane ion leakage measurement, seven leaves of each treatment were incubated in deionized water with gentle shaking overnight. The conductivity was measured before (C1) and after (C2) boiling for 10 min with an electro-conductivity meter. The ratio of C1:C2 represents the membrane ion leakage rate.

Measurement of the effective PS II quantum yield (Φ_{PSII})

For the photosynthetic efficiency, the whole plants were dark-adapted for 30 min before measurements and the Φ_{PSII} of each plant was measured using IMAGING-PAMM-series Chlorophyll Fluorometer. Minimum fluorescence intensity (F_0) was measured under a weak

ML (wavelength 650 nm). A saturating pulse (SP) of red light (5000 μmol photons m^{-2} s^{-1}, for 0.8s) was applied to the leaf to estimate the maximum fluorescence in the dark-adapted state (Fm). After 40 s, the chlorophyll fluorescence curve is basically stable, and then open photochemical light AL (54 μmol photons m^{-2} s^{-1}, for 4 min). During illumination with AL, a saturating pulse (SP) of red light was applied to the leaf per 20s to estimate the maximum fluorescence (Fm'). The steady-state fluorescence (Ft) was recorded during AL illumination as well. The quantum yield of PS II [Y(II)] was calculated as Y(II) = (Fm'-Ft)/Fm'.

JA-induced leaf senescence assay

Leaf senescence assay was performed as described previously (Qi et al., 2015; Yue et al., 2012) with some modifications. The third and fourth rosette leaves from 3-week-old or 4-week-old plants were detached, rinsed in distilled water or MES buffer, and then floated on 6 mL of distilled water or MES buffer supplied with mock (add 6 μL 75% ethanol) or methyl-jasmonate (add 6 μL 0.1 M MeJA to adjust working concentration as 100 μM MeJA) and kept in dark at 22 °C for 3 d to 5 d accordingly.

Dark-induced leaf senescence

Detached fourth and fifth rosette leaves of three-week-old plants were floated on 6 mL of distilled water, or whole plants were incubated in complete darkness with the indicated periods.

RNA-Seq analysis

For the RNA-Seq experiments, plants were grown under LD conditions at 22ºC for 10 days and harvested at ZT12. RNA-sequencing was performed by (ANNOROAD, Beijing). Sequencing libraries were generated using NEBNext®Ultra™ RNA Library Prep Kit for Illumina® (#E7530L, NEB, USA) following manufacturer's recommendations and index codes were added to attribute sequences to each sample. The clustering of the index-coded samples was performed on a cBot cluster generation system using HiSeq SR Cluster Kit v4-cBot-HS (Illumina) according to the manufacturer's instructions. After cluster generation, the libraries were sequence don an Illumina Hiseq platform and 50 bp single reads were generated. Raw data was processed with Perl scripts to ensure the quality for further analysis.

The filtering criteria are as follows：1) Remove the adaptor-polluted reads. Reads containing more than 5 adapter-polluted bases were regarded as adaptor-polluted reads and have been filtered out; 2) Remove the low-quality reads. Reads with the number of low quality bases (phred Quality value less than 19) accounting for more than 15% of total bases are regarded as low-quality reads; 3) Remove reads with number of N bases accounting for more than 5 %. As for paired-end sequencing data, both reads have been filtered out if any read of the paired-end reads are adaptor-polluted. The obtained clean data after filtering were subjected to statistical analyses to determine their quantity and quality, including Q30, data quantity and base content statistics, etc. Then high-quality reads were aligned against the *Arabidopsis thaliana* reference genome sequence (TAIR10 Genome Release) with TopHat (version2.0.12). DESeq (v1.16) was used for differential gene expression analysis using a model based on the negative binomial distribution. The *p*-value could be assigned to each gene and adjusted by the Benjamini and Hochberg's approach for controlling the false discovery rate. Genes with $q \leq 0.05$ and $|\log2\_ratio| \geq 1$ are identified as differentially expressed genes (DEGs). The GO (Gene Ontology, http://geneontology.org/) enrichment of DEGs was implemented by the hypergeometric test, in which *p*-value is calculated and adjusted as *q*-value. GO terms with $q<0.05$ were considered to be significantly enriched. The Integrative Genomics Viewer (IGV) was used to visualize the reads for selected genes (Robinson et al, 2011; Thorvaldsdottir et al, 2013).

RT-qPCR

Seedlings were grown under LD for 10 d and samples were harvested at ZT12. For the analysis of JA-induced *MYC2* expression, plants were treated with 50 μM MeJA (Aladdin) or 0.035% ethanol (Mock) for 1 h at different times of the day with 4 h interval. Total RNA was extracted using a TRIzol RNA extraction kit (Invitrogen) and treated with RNase-free DNase I (Thermo Fisher). 1 μg RNA was used to synthesize cDNA using M-MLV Reverse Transcriptase (Promega). Quantitative PCR was performed using SYBR Green Real-time PCR Master Mix (Toyobo, Osaka, Japan) according to the manufacturer's instructions on a Mx3000P instrument (Stratagene, La Jolla, CA, USA). The following PCR program was used: 95°C for 2 min, followed by 40 cycles of 95°C for 15 s, 55°C for 15 s and 72°C for 15 s,

followed by a melting-curve program. Gene expression was normalized by *ACTIN2* expression. Experiments were repeated with at least three biological and three technical replicates. Data represent means±s.d. of three technical replicates. Primers used for real-time PCR assay are listed in Supplemental Table 2.

Yeast one-hybrid analysis

For yeast one-hybrid assay, the coding sequence of *LUX* was inserted into pGAD424 to generate pGAD424-LUX. The 1,500 bp *MYC2* promoter and 2,000 bp *SAG29* and 2,000 bp *NAP* promoter were inserted into pLacZi vector to generate the *MYC2p:Pcyc1-LacZ*, *SAG29p:Pcyc1-LacZ* and *NAPp:Pcyc1-LacZ* reporter plasmid, respectively. These constructs were transformed into the *Saccharomyces cerevisiae* EGY48 strain and the X-gal staining was carried out accordingly. Transformed yeast was selected on synthetic complete medium lacking Ura and Leu (Lin et al, 2007).

Transient transcriptional activity assay in tobacco

For transcriptional activity assay in tobacco, *Agrobacterium tumefaciens* AGL carrying various fusion expression vectors (effector: GFP-LUX or GFP; reporter: *COI1pro:LUC*-1300, *JAZ1pro:LUC-1300*, *MYC2pro:LUC-1300*, *MYC4pro:LUC-1300* and *NAPpro:LUC*-1300) were cultured overnight. Each reporter vector paired with GFP-LUX or GFP effector vector were then co-transformed into tobacco leaves using a syringe infiltration method. The luciferase signal was detected using a CCD camera 2 days after infiltration. The bioluminescence intensity of LUC signals was quantified by Metamorph software.

ChIP assay

To confirm Evening Complex bind *MYC2* promoter *in vivo*, chromatin immunoprecipitation (ChIP) assay was carried out using *pELF4:ELF4-HA* and *35:GFP-LUX* transgenic plants (Zhang et al, 2013). HA and GFP antibody was used for immunoprecipitation. The DNA products of IP were analyzed by RT–qPCR. Data were presented as mean±s.d, n=3. Primers used in this assay were shown in Supplemental Table 2.

***Arabidopsis* protoplast transient expression analysis**

For transient expression assay, a 1,500 bp *MYC2* promoter and 1,055 bp *COI1* promoter were amplified to generate the *MYC2pro:LUC* and *COI1pro:LUC* reporter construct. The coding sequence of LUX was inserted into pBI221 vector under the control of the *CaMV35S* promoter. The plasmid carrying the GUS gene under the control of the *CaMV35S* promoter was used as an internal control for data normalization. The effector: reporter: GUS co-transformed to protoplast as a ratio of 5:3:2. The LUC and GUS activities were measured separately, and the LUC/GUS ratio was presented as normalized gene expression.

JA measurement

Approximately 50 mg fresh weight ground leaf tissues were extracted with 1 mL 80% MeOH/H_2O with 10 ng internal standard and shaken overnight at 4^{o}C. The samples were then centrifuged at 9,000 rpm for 5 min. The upper phase was collected and dried under streaming nitrogen and resuspended in 400 μL 5% acetic acid/ ethyl acetate and 400 μL H_2O. After blending, the samples were centrifuged at 9,000 rpm for 5 min, and the upper phase was collected and dried under streaming nitrogen and resuspended in 30 μL MeOH and 100 μL H_2O and incubated for 2 h at -20 ^{o}C. Samples were then centrifuged at 12,000 rpm for 7 min, and the upper phase was collected and dried under streaming nitrogen and resuspended in 30 μL BSTFA and 3 μL pyridine, and incubated 30 min at -80 ^{o}C. The analysis of JA constituents was performed using GC-TOF/MS Pegasus IV mass spectrometer.

Acknowledgements

We thank Dr. Daoxin Xie (Tsinghua University) for *myc2, MYC2OE* and *myc2 myc3 myc4* seeds. We are grateful for Dr. JyanChyun Jang (The Ohio State University) and Dr. Seth J Davis (University of York) 's critical comments and helpful suggestions on this study. The work was supported by the National Natural Sciences Foundation of China (31670290 and 31570292), Youth Innovation Promotion Association CAS to Y. Z. (NO. 2017110), 'Youth 1000 plan' to L.W. and the Chinese Academy of Sciences (QYZDB-SSW-SMC011 and XDTB0400-02).

Author contributions

Y.Z. and L.W. designed the project. Y.Z., Y.W., H.W., N. L. and W.T. performed the

experiments. Y.Z. and L.W. analyzed the data. Y.Z, K.C and L.W. wrote the article.

Conflict of interest

The authors declare that they have no conflict of interest.

Additional information

RNA-seq data reported in this study have been deposited in the Gene Expression Omnibus database under the accession number GSE99290.

Accession numbers

The *Arabidopsis* Genome Initiative numbers for the genes mentioned in this article are as follows: *ELF3*, AT2G25930; *ELF4*, AT2G40080; *LUX*, AT3G46640; *MYC2*, AT1G32640; *ANAC019*, AT1G52890; *ANAC055*, AT3G15500; *ANAC072*, AT4G27410; *NAP*, AT1G69490; *ORE1*, AT5G39610; *SAG29*, AT5G13170; *SAG13*, AT2G29350; *SAG113*, AT5G59220; *SEN4*, AT4G30270; *RBCS*, AT1G67090.

References

Bu, Q., Jiang, H., Li, C.B., Zhai, Q., Zhang, J., Wu, X., Sun, J., Xie, Q., and Li, C. (2008). Role of the *Arabidopsis thaliana* NAC transcription factors ANAC019 and ANAC055 in regulating jasmonic acid-signaled defense responses. Cell Res 18:756-767.

Chen, Q., Sun, J., Zhai, Q., Zhou, W., Qi, L., Xu, L., Wang, B., Chen, R., Jiang, H., Qi, J., et al. (2011). The basic helix-loop-helix transcription factor MYC2 directly represses *PLETHORA* expression during jasmonate-mediated modulation of the root stem cell niche in *Arabidopsis*. Plant Cell 23:3335-3352.

Chow, B.Y., Helfer, A., Nusinow, D.A., and Kay, S.A. (2012). ELF3 recruitment to the PRR9 promoter requires other Evening Complex members in the *Arabidopsis* circadian clock. Plant Signal Behav 7:170-173.

Covington, M.F., Maloof, J.N., Straume, M., Kay, S.A., and Harmer, S.L. (2008). Global transcriptome analysis reveals circadian regulation of key pathways in plant growth and development. Genome Biol 9:R130.

Covington, M.F., Panda, S., Liu, X.L., Strayer, C.A., Wagner, D.R., and Kay, S.A. (2001).

ELF3 modulates resetting of the circadian clock in *Arabidopsis*. Plant Cell 13:1305-1315.

Fernandez-Calvo, P., Chini, A., Fernandez-Barbero, G., Chico, J.M., Gimenez-Ibanez, S., Geerinck, J., Eeckhout, D., Schweizer, F., Godoy, M., Franco-Zorrilla, J.M., et al. (2011). The *Arabidopsis* bHLH transcription factors MYC3 and MYC4 are targets of JAZ repressors and act additively with MYC2 in the activation of jasmonate responses. Plant Cell 23:701-715.

Gan, S., and Amasino, R.M. (1995). Inhibition of leaf senescence by autoregulated production of cytokinin. Science 270:1986-1988.

Goodspeed, D., Chehab, E.W., Covington, M.F., and Braam, J. (2013). Circadian control of jasmonates and salicylates: the clock role in plant defense. Plant Signal Behav 8:e23123.

Goodspeed, D., Chehab, E.W., Min-Venditti, A., Braam, J., and Covington, M.F. (2012). *Arabidopsis* synchronizes jasmonate-mediated defense with insect circadian behavior. Proc Natl Acad Sci USA 109:4674-4677.

Greenham, K., and McClung, C.R. (2015). Integrating circadian dynamics with physiological processes in plants. Nat Rev Genet 16:598-610.

Guo, Y., and Gan, S. (2006). AtNAP, a NAC family transcription factor, has an important role in leaf senescence. Plant J 46:601-612.

He, Y., Fukushige, H., Hildebrand, D.F., and Gan, S. (2002). Evidence supporting a role of jasmonic acid in *Arabidopsis* leaf senescence. Plant Physiol 128:876-884.

Helfer, A., Nusinow, D.A., Chow, B.Y., Gehrke, A.R., Bulyk, M.L., and Kay, S.A. (2011). *LUX ARRHYTHMO* encodes a nighttime repressor of circadian gene expression in the *Arabidopsis* core clock. Curr Biol 21:126-133.

Herrero, E., Kolmos, E., Bujdoso, N., Yuan, Y., Wang, M., Berns, M.C., Uhlworm, H., Coupland, G., Saini, R., Jaskolski, M., et al. (2012). EARLY FLOWERING4 recruitment of EARLY FLOWERING3 in the nucleus sustains the *Arabidopsis* circadian clock. Plant Cell 24:428-443.

Hortensteiner, S. (2006). Chlorophyll degradation during senescence. Annual review of plant biology 57:55-77.

Hsu, P.Y., and Harmer, S.L. (2014). Wheels within wheels: the plant circadian system. Trends Plant Sci 19:240-249.

Ingle, R.A., Stoker, C., Stone, W., Adams, N., Smith, R., Grant, M., Carre, I., Roden, L.C., and Denby, K.J. (2015). Jasmonate signalling drives time-of-day differences in susceptibility of *Arabidopsis* to the fungal pathogen *Botrytis cinerea*. Plant J 84:937-948.

Kim, W.Y., Hicks, K.A., and Somers, D.E. (2005). Independent roles for EARLY FLOWERING 3 and ZEITLUPE in the control of circadian timing, hypocotyl length, and flowering time. Plant Physiol 139:1557-1569.

Lee, H.G., Mas, P., and Seo, P.J. (2016). MYB96 shapes the circadian gating of ABA signaling in *Arabidopsis*. Sci Rep 6:17754.

Li, Z., Zhao, Y., Liu, X., Peng, J., Guo, H., and Luo, J. (2014). LSD 2.0: an update of the leaf senescence database. Nucleic Acids Res 42:D1200-1205.

Lim, P.O., Kim, H.J., and Nam, H.G. (2007). Leaf senescence. Annual review of plant biology 58:115-136.

Lin, R., Ding, L., Casola, C., Ripoll, D.R., Feschotte, C., and Wang, H. (2007). Transposase-derived transcription factors regulate light signaling in *Arabidopsis*. Science 318:1302-1305.

Liu, X.L., Covington, M.F., Fankhauser, C., Chory, J., and Wagner, D.R. (2001). *ELF3* encodes a circadian clock-regulated nuclear protein that functions in an *Arabidopsis* PHYB signal transduction pathway. Plant Cell 13:1293-1304.

Miao, Y., and Zentgraf, U. (2007). The antagonist function of *Arabidopsis* WRKY53 and ESR/ESP in leaf senescence is modulated by the jasmonic and salicylic acid equilibrium. Plant Cell 19:819-830.

Mishra, K.B., Mishra, A., Novotna, K., Rapantova, B., Hodanova, P., Urban, O., and Klem, K. (2016). Chlorophyll a fluorescence, under half of the adaptive growth-irradiance, for high-throughput sensing of leaf-water deficit in *Arabidopsis thaliana* accessions. Plant Methods 12:46.

Mizuno, T., Kitayama, M., Takayama, C., and Yamashino, T. (2015). Insight into a Physiological Role for the EC Night-Time Repressor in the *Arabidopsis* Circadian Clock. Plant Cell Physiol 56:1738-1747.

Mizuno, T., Nomoto, Y., Oka, H., Kitayama, M., Takeuchi, A., Tsubouchi, M., and Yamashino, T. (2014). Ambient temperature signal feeds into the circadian clock

transcriptional circuitry through the EC night-time repressor in *Arabidopsis thaliana*. Plant Cell Physiol 55:958-976.

Mockler, T.C., Michael, T.P., Priest, H.D., Shen, R., Sullivan, C.M., Givan, S.A., McEntee, C., Kay, S.A., and Chory, J. (2007). The DIURNAL project: DIURNAL and circadian expression profiling, model-based pattern matching, and promoter analysis. Cold Spring Harb Sym 72:353-363.

Nieto, C., Lopez-Salmeron, V., Daviere, J.M., and Prat, S. (2015). ELF3-PIF4 interaction regulates plant growth independently of the Evening Complex. Curr Biol 25:187-193.

Nusinow, D.A., Helfer, A., Hamilton, E.E., King, J.J., Imaizumi, T., Schultz, T.F., Farre, E.M., and Kay, S.A. (2011). The ELF4-ELF3-LUX complex links the circadian clock to diurnal control of hypocotyl growth. Nature 475:398-402.

Park, J.H., Oh, S.A., Kim, Y.H., Woo, H.R., and Nam, H.G. (1998). Differential expression of senescence-associated mRNAs during leaf senescence induced by different senescence-inducing factors in *Arabidopsis*. Plant Mol Biol 37:445-454.

Qi, T., Wang, J., Huang, H., Liu, B., Gao, H., Liu, Y., Song, S., and Xie, D. (2015). Regulation of Jasmonate-Induced Leaf Senescence by Antagonism between bHLH Subgroup IIIe and IIId Factors in *Arabidopsis*. Plant Cell 27:1634-1649.

Qiu, K., Li, Z., Yang, Z., Chen, J., Wu, S., Zhu, X., Gao, S., Gao, J., Ren, G., Kuai, B., et al. (2015). EIN3 and ORE1 accelerate degreening during ethylene-mediated leaf senescence by directly activating chlorophyll catabolic genes in *Arabidopsis*. PLoS Genet 11:e1005399.

Rauf, M., Arif, M., Dortay, H., Matallana-Ramirez, L.P., Waters, M.T., Gil Nam, H., Lim, P.O., Mueller-Roeber, B., and Balazadeh, S. (2013). ORE1 balances leaf senescence against maintenance by antagonizing G2-like-mediated transcription. EMBO Rep 14:382-388.

Robinson, J.T., Thorvaldsdottir, H., Winckler, W., Guttman, M., Lander, E.S., Getz, G., and Mesirov, J.P. (2011). Integrative genomics viewer. Nat Biotechnol 29:24-26.

Sakuraba, Y., Jeong, J., Kang, M.Y., Kim, J., Paek, N.C., and Choi, G. (2014). Phytochrome-interacting transcription factors PIF4 and PIF5 induce leaf senescence in *Arabidopsis*. Nat Commun 5:4636.

Sanchez, S.E., and Kay, S.A. (2016). The plant circadian clock: from a simple timekeeper to a complex developmental manager. Cold Spring Harb Perspect Biol.

Shan, X., Wang, J., Chua, L., Jiang, D., Peng, W., and Xie, D. (2011). The role of *Arabidopsis* Rubisco activase in jasmonate-induced leaf senescence. Plant physiol 155:751-764.

Shin, J., Heidrich, K., Sanchez-Villarreal, A., Parker, J.E., and Davis, S.J. (2012). TIME FOR COFFEE represses accumulation of the MYC2 transcription factor to provide time-of-day regulation of jasmonate signaling in *Arabidopsis*. Plant Cell 24:2470-2482.

Thines, B., Katsir, L., Melotto, M., Niu, Y., Mandaokar, A., Liu, G., Nomura, K., He, S.Y., Howe, G.A., and Browse, J. (2007). JAZ repressor proteins are targets of the SCF(COI1) complex during jasmonate signalling. Nature 448:661-665.

Thorvaldsdottir, H., Robinson, J.T., and Mesirov, J.P. (2013). Integrative Genomics Viewer (IGV): high-performance genomics data visualization and exploration. Brief Bioinform 14:178-192.

Weaver, L.M., Gan, S., Quirino, B., and Amasino, R.M. (1998). A comparison of the expression patterns of several senescence-associated genes in response to stress and hormone treatment. Plant Mol Biol 37:455-469.

Wu, X.Y., Kuai, B.K., Jia, J.Z., and Jing, H.C. (2012). Regulation of leaf senescence and crop genetic improvement. J Integr Plant Biol 54:936-952.

Xie, D.X., Feys, B.F., James, S., Nieto-Rostro, M., and Turner, J.G. (1998). COI1: an *Arabidopsis* gene required for jasmonate-regulated defense and fertility. Science 280:1091-1094.

Xu, L., Liu, F., Lechner, E., Genschik, P., Crosby, W.L., Ma, H., Peng, W., Huang, D., and Xie, D. (2002). The SCF(COI1) ubiquitin-ligase complexes are required for jasmonate response in *Arabidopsis*. Plant Cell 14:1919-1935.

Yu, J.W., Rubio, V., Lee, N.Y., Bai, S., Lee, S.Y., Kim, S.S., Liu, L., Zhang, Y., Irigoyen, M.L., Sullivan, J.A., et al. (2008). COP1 and ELF3 control circadian function and photoperiodic flowering by regulating GI stability. Mol Cell 32:617-630.

Yue, H., Nie, S., and Xing, D. (2012). Over-expression of *Arabidopsis* Bax inhibitor-1 delays methyl jasmonate-induced leaf senescence by suppressing the activation of MAP kinase 6. J Exp Bot 63:4463-4474.

Zhang, Y., Li, B., Xu, Y., Li, H., Li, S., Zhang, D., Mao, Z., Guo, S., Yang, C., Weng, Y., et

al. (2013). The cyclophilin CYP20-2 modulates the conformation of BRASSINAZOLE-RESISTANT1, which binds the promoter of *FLOWERING LOCUS D* to regulate flowering in *Arabidopsis*. Plant Cell 25:2504-2521.

Zhao, Y., Chan, Z., Gao, J., Xing, L., Cao, M., Yu, C., Hu, Y., You, J., Shi, H., Zhu, Y., et al. (2016). ABA receptor PYL9 promotes drought resistance and leaf senescence. Proc Natl Acad Sci USA 113:1949-1954.

Zhu, X., Chen, J., Xie, Z., Gao, J., Ren, G., Gao, S., Zhou, X., and Kuai, B. (2015). Jasmonic acid promotes degreening via MYC2/3/4- and ANAC019/055/072-mediated regulation of major chlorophyll catabolic genes. Plant J 84:597-610.

Figure Legends

Figure 1. Precocious leaf senescence in EC mutants.

(A) The senescence phenotypes of 5-week-old plants. Arrows indicate senescent leaves.

(B) Chlorophyll a fluorescence analysis indicated early senescence in EC mutants. Arrows indicate senescent leaves.

(C) Chlorophyll a fluorescence parameters Φ_{PSII} measurements. Error bars represent SE (n>24).

(D-E) Chlorophyll content (**D**) and ion leakage (**E**) in the third and fourth leaves of different plants. The chlorophyll content of EC mutants are relative to Col-0, which was set as 100. For ion leakage measurement, the conductivity was measured before (C1) and after (C2) boiling for 10 min with an electro-conductivity meter. The ratio of C1:C2*100 represents the membrane ion leakage rate. Three biological replicates were performed. Error bars represent SD.

(F-H) Quantitative real-time PCR analysis for photosynthetic gene *RBCS* (**F**), *CAB1* (**G**) and senescence associate gene *SAG12* **(H)** of the senescent leaves, using *ACTIN2* as an internal control. *Y axis* is calculate with this formula $2^{-\triangle[CT(GENE)-CT(ACTIN2)]}$. Three biological replicates were performed for Figure F-G and four biological replicates were performed for Figure H. Error bars represent SD. * and ** indicate significant difference in comparison with Col-0 at $p<0.05$ and $p<0.01$ (*t*-test), respectively.

Figure 2. Transcriptome profiling analyses link EC to JA signaling.

(A) Differential Expressed Genes (DEGs) between *lux-6* and wild-type Col-0.

(B) Functional assignment of the DEGs by GO analysis, bar represents *q* value.

(C) Overlap of up-regulated DEGs with leaf senescence regulatory genes (SRGs). Fisher's exact test was used to calculate the *p*-value. Heatmap shows up-regulated SRGs in *lux-6*. Scale represents fold change.

(D) Overlap of DEGs in *lux-6* with JA-responsive genes. Fisher's exact test was used to calculate the p-value. Heatmap shows up-regulated JA-responsive genes in *lux-6*. Scale represents fold change.

(E-F) Visualization of RNA-seq coverage profiles for *MYC2*, *ANAC019*, *ANAC055* and *ANAC072* by using Integrative Genomics Viewer (IGV) browser. Scale represents reads counts.

Figure 3. Circadian EC components modulate JA-induced leaf senescence.

(A) The third and fourth rosette leaves from 3-week-old plants were detached and senescence phenotypes of detached leaves treated with mock or 100 μM MeJA in the dark for 60 h.

(B-C) Chlorophyll (**B**) and ion leakage (**C**) measurement of the detached leaves as shown in (**A**). The chlorophyll content in the Col-0 with Mock treatment was defined as 100. One sample t-test was used for this analysis. For ion leakage measurement, the conductivity was measured before (C1) and after (C2) boiling for 10 min with an electro-conductivity meter. The ratio of C1:C2*100 represents the membrane ion leakage rate. Three biological replicates were performed. Error bars represent SD.

(D-H) Quantitative real-time PCR analysis of *SAG13* (**D**), *SAG29* (**E**), *SAG113* (**F**), and *SEN4* (**G**) and photosynthetic gene *RBCS* (**H**) from detached leaves as shown in (**A**), using *ACTIN2* as an internal control. *Y axis* is calculate with this formula $2^{-\triangle[CT(GENE)-CT(ACTIN2)]}$. Three biological replicates were performed. Error bars represent SD. * and ** indicate significant difference in comparison with Col-0 at $p<0.05$ and $p<0.01$ (*t*-test), respectively.

Figure 4. *ELF3 OE* attenuates JA-induced leaf senescence.

(A) The third and fourth rosette leaves from 3-week-old plants were detached and senescence phenotypes of detached leaves treated with mock or 100 μM MeJA in the dark for 96 h.

(B-C) Chlorophyll (**B**) and ion leakage (**C**) measurement of the detached leaves as shown in (**A**). The chlorophyll content in the Col-0 with Mock treatment was defined as 100. One sample t-test was used for this analysis. For ion leakage measurement, the conductivity was measured before (C1) and after (C2) boiling for 10 min with an electro-conductivity meter. The ratio of C1:C2*100 represents the membrane ion leakage rate.

(D-H) Quantitative real-time PCR analysis of *SAG13* (**D**), *SAG29* (**E**), *SAG113* (**F**), and *SEN4* (**G**) and photosynthetic gene *RBCS* (**H**) from detached leaves as shown in (**A**), using *ACTIN2*

as an internal control. *Y axis* is calculate with this formula $2^{-\triangle[CT(GENE)-CT(ACTIN2)]}$. Three biological replicates were performed. Error bars represent SD. * and ** indicate significant differences in comparison with Col-0 at $p<0.05$ and $p<0.01$ (*t*-test), respectively.

Figure 5. LUX binds *MYC2* promoter and repress its expression.

(A) Bioluminescence of co-transformation of either *GFP* or *35S:GFP-LUX* (GFP-LUX) with *MYC2p:LUC*, *COI1p:LUC*, *JAZ1p:LUC* and *MYC4p:LUC* in *N. benthamiana*. Shown are representatives of three trials with similar results.

(B) Quantification of bioluminescence intensity as shown in (**A**). The relative bioluminescence intensity in the tobacco leaves co-transformed with GFP and reporter vector was defined as 100. Bar represents SE. (n>7).

(C) Transcriptional repression activity assay in *Arabidopsis* protoplast transient expression analysis. *COI1pro:LUC* and *35S:GUS* were used as a negative and internal control, respectively. The effector: reporter: GUS co-transformed to protoplast as a ratio of 5:3:2. The relative LUC/GUS activity in the protoplast co-transformed with GFP and reporter vector was defined as 1. Three biological replicates were performed. Error bars represent SE.

(D) Yeast one-hybrid analysis. The coding sequence of *LUX* was inserted into pGAD424 to generate pGAD424-LUX. The 1,500 bp *MYC2* promoter and 2,000 bp *SAG29* promoter were inserted into pLacZi vector to generate *MYC2p:Pcyc1-LacZ* and *SAG29p:Pcyc1-LacZ* reporter, respectively. Blue color from X-gal staining indicating LUX binding.

(E) Chromatin immunoprecipitation assay using Col-0, *ELF4pro:ELF4-HA* and *35S:GFP-LUX* plants. Schematic representation on top indicates the locations of amplicons for ChIP analysis on *MYC2* promoter. Three biological replicates were performed. Error bars represent SD. * and ** indicate significant differences in comparison with Col-0 at $p<0.05$ and $p<0.01$ (*t*-test), respectively.

Figure 6. The IIIebHLH factors are required for EC-mediated control of leaf senescence induced by JA.

(A) The *myc2-2* could revert *elf3-1* fast leaf senescence phenotypes. The third and fourth rosette leaves from 3-week-old plants were detached and senescence phenotypes of detached leaves treated with mock or 100 μM MeJA in the dark for 60 h.

(B-C) Chlorophyll (**B**) and ion leakage (**C**) measurement of detached leaves as shown in (**A**). The chlorophyll content in the Col-0 with Mock treatment was defined as 100. One sample t-test was used for this analysis. For ion leakage measurement, the conductivity was measured before (C1) and after (C2) boiling for 10 min with an electro-conductivity meter. The ratio of C1:C2*100 represents the membrane ion leakage rate. Three biological replicates were performed. Error bars represent SD.

(D) The *myc2 myc3 myc4* could revert *lux-6* fast leaf senescence phenotypes. The third and fourth rosette leaves from 3-week-old plants were detached and senescence phenotypes of detached leaves treated with mock or 100 μM MeJA in the dark for 4 d.

(E-F) Chlorophyll (**E**) and ion leakage (**F**) measurement of the detached leaves as shown in (**D**). The chlorophyll content in the Col-0 with Mock treatment was defined as 100. For ion leakage measurement, the conductivity was measured before (C1) and after (C2) boiling for 10 min with an electro-conductivity meter. The ratio of C1:C2*100 represents the membrane ion leakage rate. Three biological replicates were performed. Error bars represent SD. Different letters indicate significant differences by one-way ANOVA analysis with SPSS statistics software (p<0.05). Capital letters compare with each other, and lowercase letters compare with each other.

Figure 7. Proposed model for EC-mediated leaf senescence in *Arabidopsis.*

(A) JA accumulation was reduced in EC mutants. Plants were grown under 12-h light/12-h dark condition for 10 d. Tissues were harvested at ZT8. Five biological replicates were performed. Error bars represent SD. * and ** indicate significant differences in comparison with Col-0 at p<0.05 and p<0.01 (t-test), respectively.

(B) Model of the role of circadian Evening Complex in repressing jasmonate-induced leaf senescence. MYC2 acts as a positive regulator of senescence via activating its direct target genes such as *SAG29*, *PAO* and *ANAC019/055/072*. The Evening Complex directly binds to the *MYC2* promoter and represses its transcription to modulate JA-induced leaf senescence.

Maybe, EC also exhibits a feedback regulation on JA production and *JAZ1* expression to indirectly balance the JA signaling pathway.

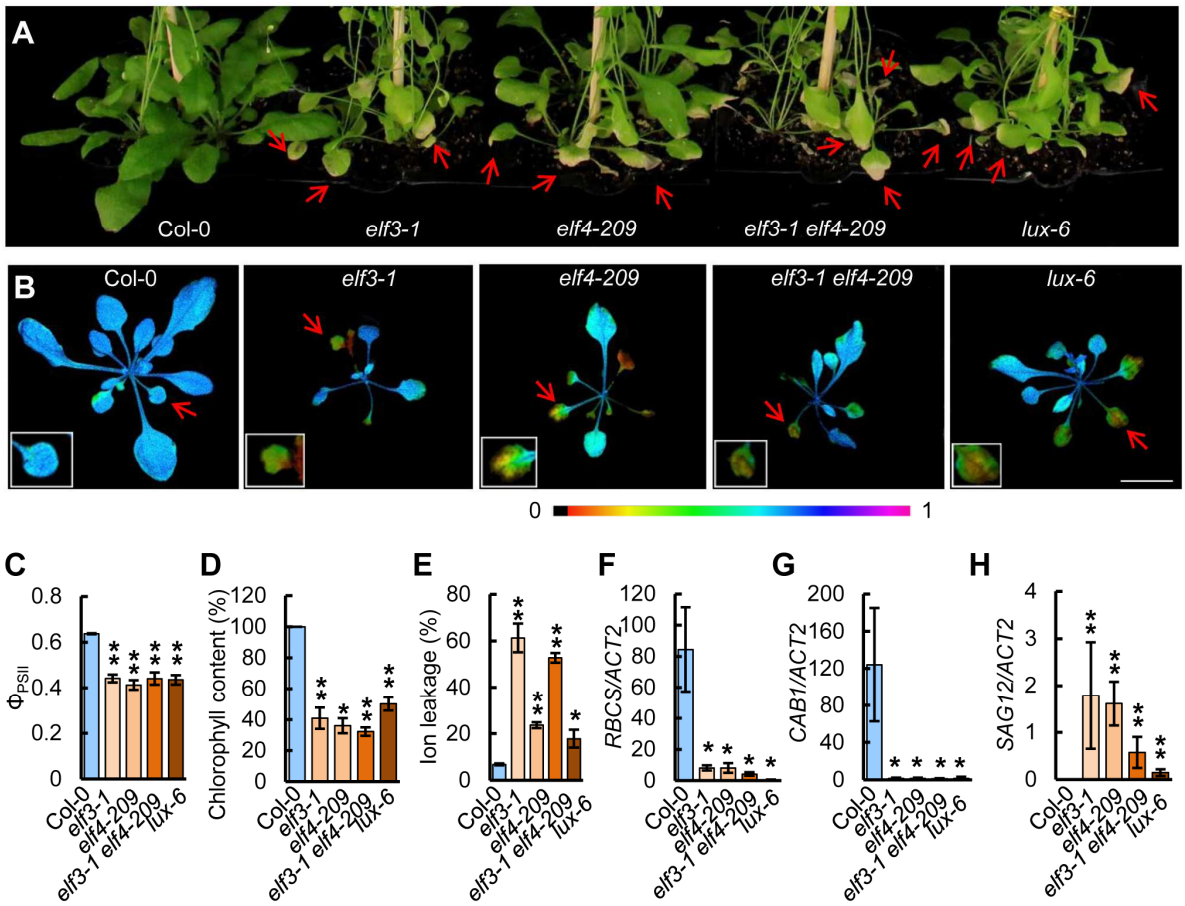

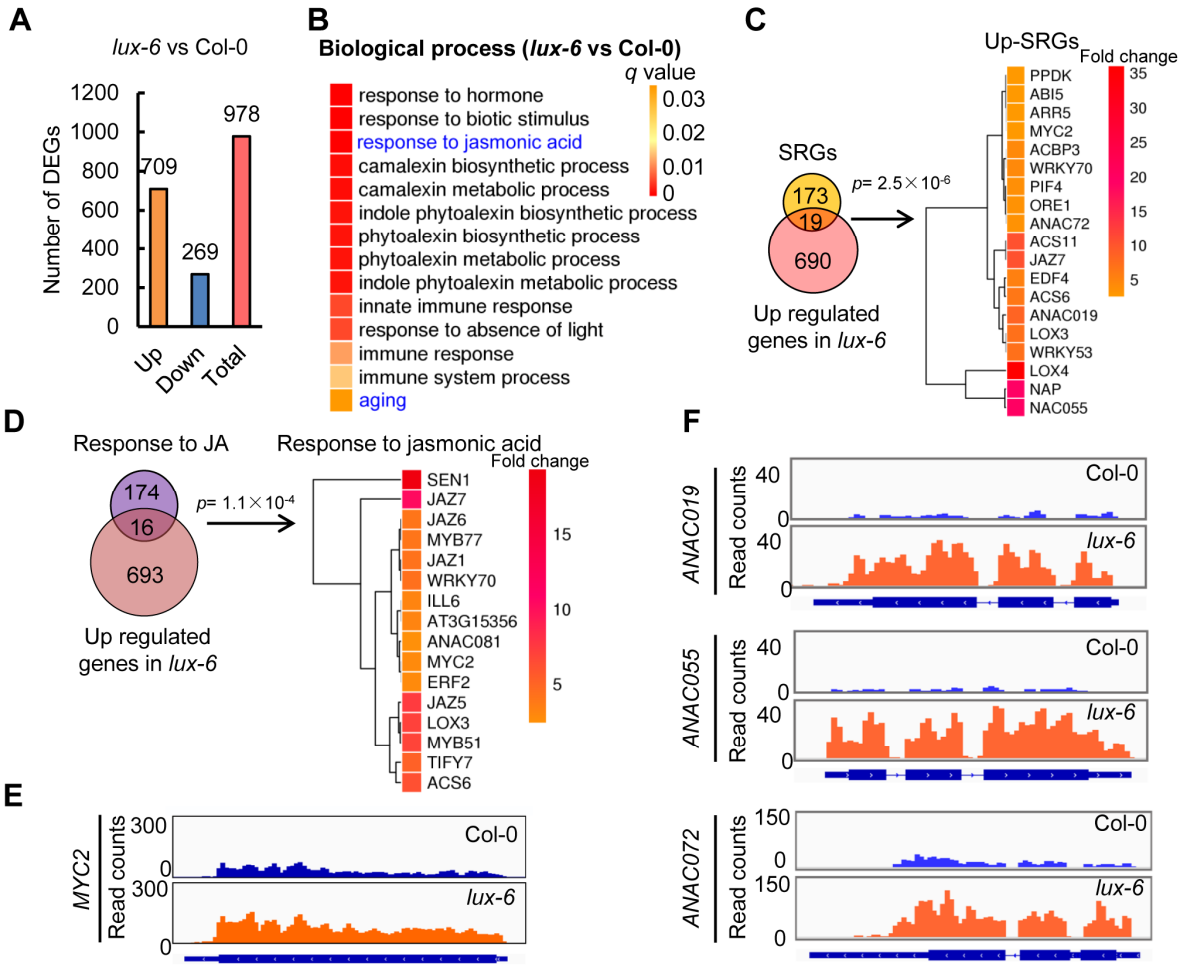

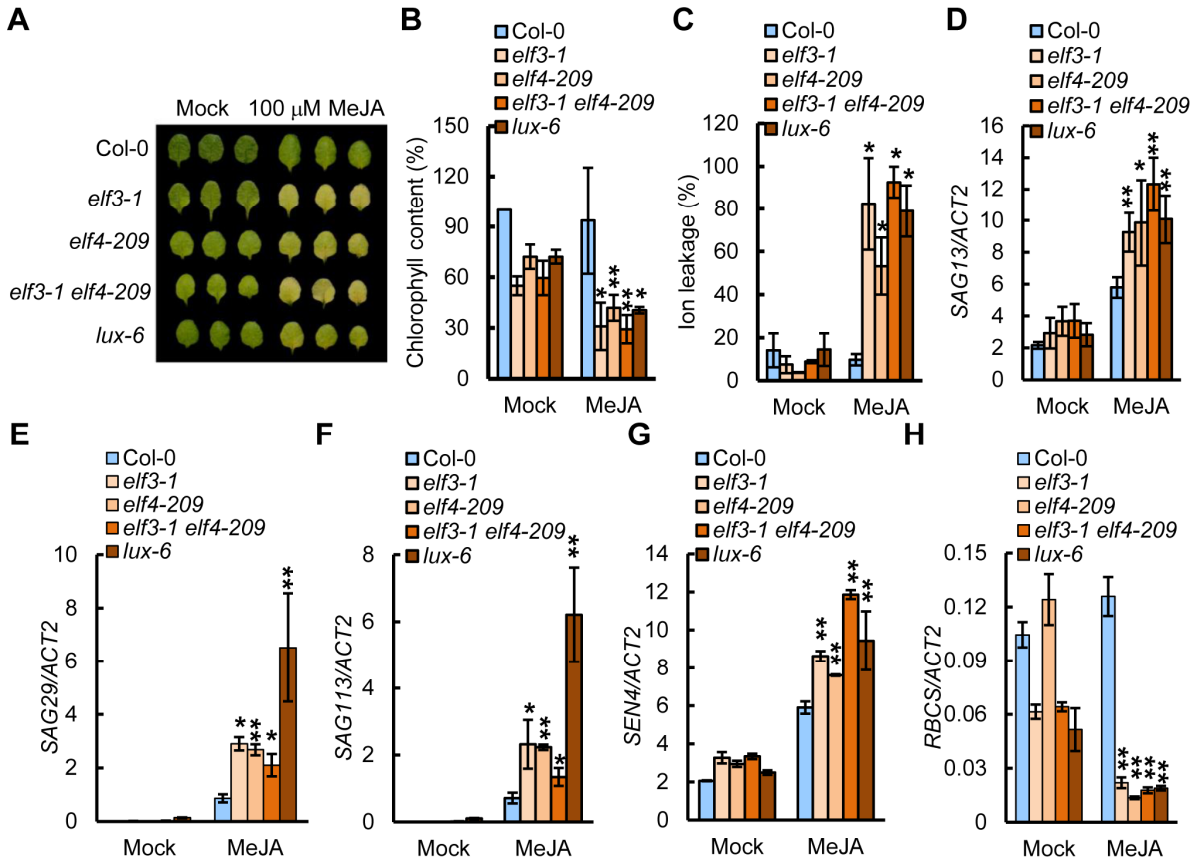

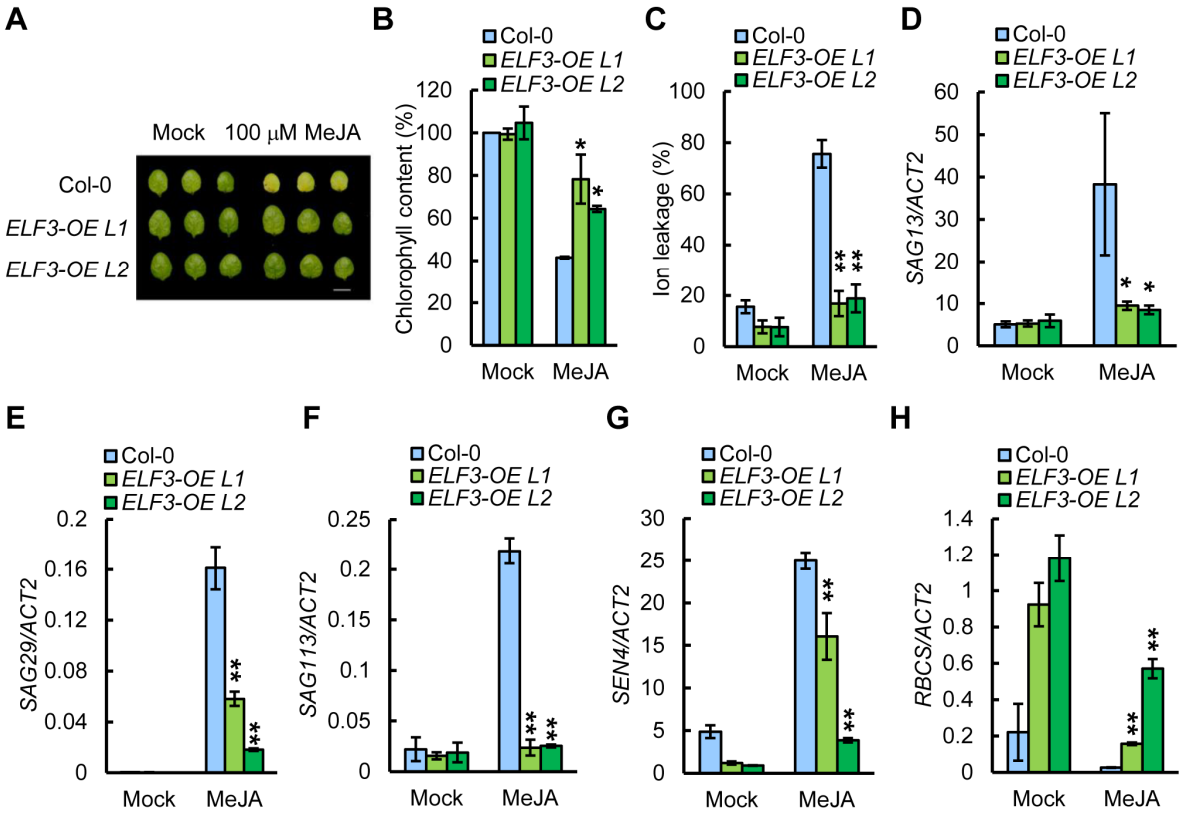

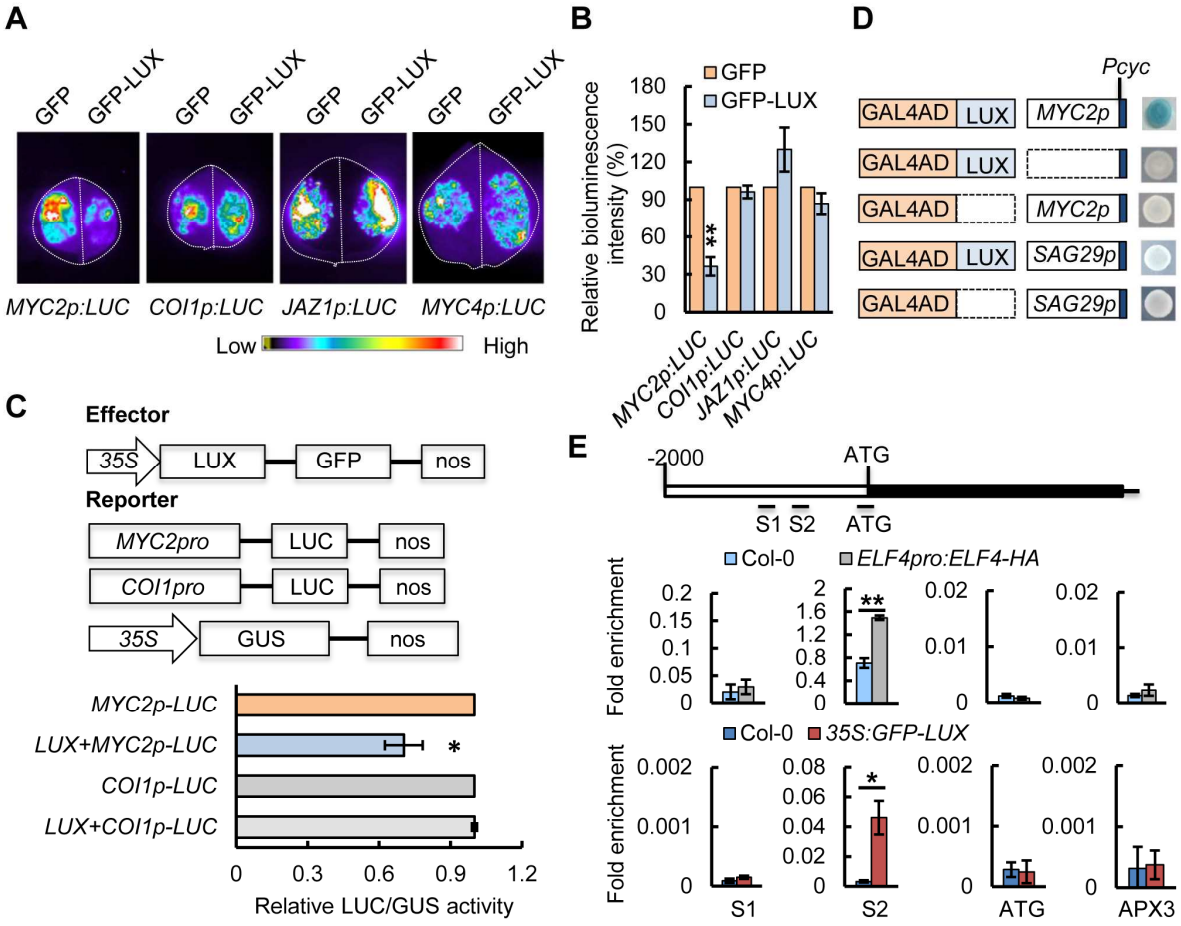
A
GFP
GFP-LUX
MYC2p:LUC
COI1p:LUC
JAZ1p:LUC
MYC4p:LUC
Low
High
B
GFP
GFP-LUX
Relative bioluminescence intensity (%)
180
150
120
90
60
30
0
**
MYC2p:LUC
COI1p:LUC
JAZ1p:LUC
MYC4p:LUC
D
Pcyc
GAL4AD
LUX
MYC2p
SAG29p
C
Effector
35S
LUX
GFP
nos
Reporter
MYC2pro
COI1pro
LUC
GUS
MYC2p-LUC
LUX+MYC2p-LUC
COI1p-LUC
LUX+COI1p-LUC
*
0
0.3
0.6
0.9
1.2
Relative LUC/GUS activity
E
-2000
ATG
S1
S2
Col-0
ELF4pro:ELF4-HA
Fold enrichment
0.2
0.15
0.1
0.05
2
1.6
1.2
0.8
0.4
0.02
0.01
35S:GFP-LUX
0.08
0.06
0.04
0.002
0.001
APX3